Received October 28, 2020, accepted November 11, 2020, date of publication November 25, 2020,
date of current version December 9, 2020.

Digital Object Identifier 10.1109/ACCESS.2020.3040534

Improved Availability Index for Repairable Fuzzy Multi-State Systems

GUAN-LIANG CHEN[1], CHUN-HO WANG[1], AND CHAO-HUI HUANG[2]
[1]Chung Cheng Institute of Technology, National Defense University, Taoyuan 335009, Taiwan
[2]Department of Applied Science, R.O.C. Naval Academy, Kaohsiung 813205, Taiwan

Corresponding author: Chao-Hui Huang (a0970437433@gmail.com)

ABSTRACT Fuzzy multi-state systems (FMSSs) comprise FMS components (FMSCs) aims at analyzing non-probabilistic uncertain circumstances defined by fuzzy state-transition rate and performance numbers. The triangular fuzzy number that features intuitive and algebraic operations is widely used for quantifying fuzziness. This study aims to overcome the drawbacks of the existing FMSS availability index that either does not conform to a normal convex set or is inconsistent with the crisp-circumstance multi-state system (MSS) availability beyond summation over state probabilities that do no equal unity. The proposed method first evaluates the instantaneous state probability (ISP) of FMSCs by establishing the FMSCs Markov model. Subsequently, the FMSSs ISP is evaluated by integrating the FMSCs ISP using the fuzzy universal generating function based on the system-structure function. A ''constrained nonlinear parameter programming model'' has been developed to evaluate the improved FMSSs availability. The corresponding availability index features the normal convex set whilst fulfilling the MSS theory, which requires state probabilities to equal unity during availability evaluation. The effectiveness of the proposed approach has been verified using an illustrated community-based smart-grid system comprising three FMSCs—solar- and wind-energy systems as well as diesel-generator equipment. Moreover, the results of an independent sensitive analysis provide further insights into the improved FMSSs availability with regard to the time and circumstance fuzziness.

INDEX TERMS Fuzzy Markov model, fuzzy multi-state availability, smart-grid system.

I. INTRODUCTION

Availability is a measure of the quality of systems and/or products, such as mobile phones, vehicles, and televisions, which find regular use. Owing to advancements in modern technology, the components used in the development of such systems and products have become affordable in terms of their environmental impacts, internal wear, corrosion, etc. However, the use of conventional binary-state reliability models may result in an inappropriate description of the dynamic performance of complex systems. An apt example of this is the performance evaluation of a power-generation system under several operating conditions, including low, normal, and high loads as well as failure or outage. Such systems feature multiple states characterized by degraded performance. Moreover, a combination of subsystems or component states existing within a system may also exhibit multi-state performance distribution. Studies concerning the development of a reliability model for multi-state systems (MSSs) have attracted increased attention in recent times [1]–[3]. Lisnianski *et al*. [4] pointed out the complications involved in the evaluation of MSS effectiveness owing to an increase in the number of components and degraded states involved in a complex MSS configuration. Some of these components and states include parallel multi-state component (MSC) systems, k-out-of-n MSSs, and MSSs with standbys. Kaul *et al*. [5] used dynamic Bayesian networks to evaluate a k-out-of-n MSS and suggested that the difficulties in solving these models must be overcome as the MSCs increase in an MSS. Fang *et al.* [6] employed a discrete continuous-time Markov chain to determine the performance of an engine capable of operating under four distinct output-energy states. The performance indicators considered in their study included the power-interruption rate and expected capacity deficiency. Manesh *et al*. [7] improved the calculation efficiency of a complex system by simplifying its

The associate editor coordinating the review of this manuscript and approving it for publication was Aniruddha Datta.

state–space diagram before applying the Markov methodology to a complex cogeneration system. The improved Markov approach has proven to be efficient at state-probability prediction and availability calculation among other indicators. Other extant studies [4], [8], [9] have proposed the use of a solution strategy that combines the universal generating function (UGF) with MSC Markov models to determine the dynamic performance of MSSs based on system-structure functions. Their proposed strategy, which avoids directly solving complex, large-scale stochastic MSS models, exclusively uses easy-to-solve stochastic MSC models combined with UGFs involving simple algebraic operations. Accordingly, a model to evaluate the reliability indicators for an MSS can be easily established. However, it is essential to gain insights into additional aspects, such as the failure principle, life prediction, and means to extend MSS life.

For scenarios with non-probabilistic uncertainties in MSSs, access to crisp reliability-related observations is impractical. Therefore, MSS performance can be more precisely quantified using fuzzy MSS reliability models compared to its conventional counterpart. Non-probabilistic uncertainty is attributable to two main factors. First, complicated MSSs degenerate with time. In the interim, the embedded components suffer several shock damages when operating in a dynamic environment. This makes the failure rates uncertain with fuzzy randomness. Secondly, with the advancement in technology, product-development-cycle durations have been significantly shortened while product lifespans have extended exponentially. Owing to time and budget restrictions, some complex systems are commercialized even before undergoing appropriate checks to meet reliability benchmarks. Such phenomena make it difficult or impossible to obtain sufficient amounts of accurate data. For example, the smart-grid system involves extensive use of wind, solar, tidal, geothermal, and other renewable energy resources. Therefore, using the MSS feature of crisp observations lowers the inferred reliability. Ding *et al*. [10] pioneered the development of a fuzzy multi-state system (FMSS) model that incorporates relative cardinality into the developed fuzzy universal generating function (FUGF). Accordingly, their proposed model quantifies the extent to which system performance meets mission demand to establish an FMSS reliability index that features linearly triangular fuzzy numbers (TFN). Liu *et al*. [11] further considered the α-cut effect to improve the method proposed in [10]. Subsequently, Hu a*et al*. [12] applied the approach proposed by Liu *et al*. [11] to a reparable FMSS. Further, Hu *et al*. [13] calculated the FMSS reliability of a discrete time-repairable MSS using trapezoidal fuzzy numbers based on the approach presented in [11]. Javid *et al*. [14] focused on the special structure of ready-to-use systems to propose a reliability model based on the Markov models and fuzzy theory. The effectiveness of their model was verified using a system in its design stage. Gao *et al*. [15] considered the system workload and degradation intensity of components to establish their FMSS reliability model. Considering an MSS with multiple uncertain signals, Dong *et al*. [16] introduced the standard interval fuzzy theory to expand the FUGF applicability. Wang *et al*. [17] proposed a novel approach to analyze the reliability of complex MSSs using trapezoidal fuzzy numbers. They used a Bayesian-network-based parameter-planning model employing fuzzy mathematics and the gray theory. Hu *et al*. [18] employed the probability and uncertainty theories to define MSS features with random uncertainty. In their research, the state probability and system-component performances were considered non-probabilistic uncertain variables, and subsequently, the uncertain UGF was used to evaluate the MSS reliability with random uncertainty. Gao *et al*. [19] considered the master–slave relationship between components to expand FUGF applicability in FMSS reliability models. Roy *et al*. [20] evaluated the reliability of wind-power devices using TFNs related to the failure- and repair-rate uncertainties, which are mainly attributable to the randomness of natural resources. They proposed a fuzzy Markov reward model whilst stating that traditional Markov reward models tend to underestimate the mean wind-power availability. Additionally, they reported MSS reliability models to be more accurate compared to their binary counterparts when evaluating wind-power reliability, notwithstanding the difficulty involved in model construction and performing calculations.

In summary, the FMSS reliability models reported in [13], [15], [16], [18]–[20] are based on the approach proposed by Ding *et al*. [10], whereas those presented in [12] and [13] are an application of the approach presented in [11] involving the use of an FMSS reliability index to compensate for the drawbacks of the method presented in [10] that utilizes linear TFN to quantify circumstances with non-probabilistic uncertainties. The approach proposed in [11] considers the α-cut value in determining the extent to which the state-performance membership function meets the mission demand. The FMSS reliability can be determined using an established linear parameter-planning model subject to summation over unit probability values. However, the fuzzy principle of normal convex sets cannot be satisfied mathematically. Most prior applications of FMSS reliability models are based on the approaches presented in [10] and [11]. Both of these approaches that either does not conform to a normal convex set or is inconsistent with the crisp-circumstance multi-state system (MSS) availability beyond summation over state probabilities that do no equal unity can be further improved. Accordingly, this paper presents an improved availability index for reparable FMSSs. In addition to considering the influence of the α-cut level on the fuzzy availability interval, the proposed method features the ''constrained nonlinear parameter-planning model'' to determine FMSS availability. The objective function of the said model measures FMSS availability as optimized state probabilities, which are normalized to ensure summation over unit probability values. Application of a linear constraint results in the attainment of linear TFNs for the availability membership functions with

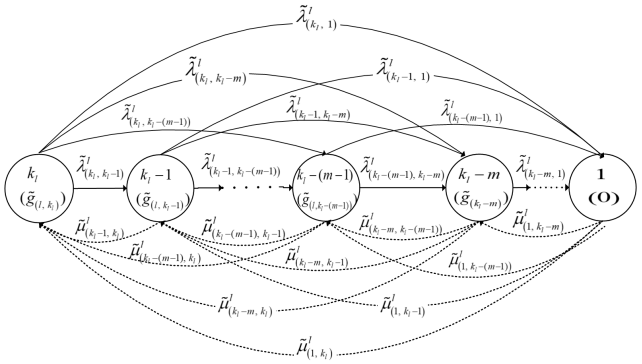

FIGURE 1. State-transition diagram for reparable FMSC.

the Karush–Kuhn–Tucker (KKT) conditions satisfied [21]. Therefore, improved FMSS availability can be optimized.

The rest of this paper is organized as follows. In Section II, the preliminaries of the fuzzy Markov stochastic process and FUGF are reviewed. The improved FMSS availability index is explained in section III. Section IV describes the efficacy of the proposed approach, determined through availability analysis of a smart-grid system. Section V presents the sensitivity analysis results to further verify the correctness and effectiveness of the proposed approach. Finally, we present the conclusions in section VI.

II. FUZZY MARKOV STOCHASTIC PROCESS AND FUZZY UNIVERSAL GENERATING FUNCTION

Typical FMSS configurations comprise series, parallel, and series–parallel systems, the state-transition rates and performances of which are fuzzy numbers. The FMSS models proposed by Liu *et al.* [11] and Hu *et al.* [12] employ a typical series–parallel configuration comprising several fuzzy multi-state components (FMSCs). TFN, which features intuitive and algebraic operations, is extensively employed to measure FMSC-circumstance fuzziness pertaining to the state-transition intensity and MSS performance [10]–[12], [15], [19], [20]. Initially, FMSCs degrade from their best to worse states over time. However, through appropriate maintenance, they can be restored to previous better states. Fig. 1 depicts the fuzzy state-transition diagram of the l^{th} FMSC in a reparable FMSS. The term $\tilde{\lambda}^{l}_{(i,j)}$ $(i, j = 1, 2, \ldots, k_l, i > j)$ represents the fuzzy number for the said FMSCs degradation rate from a high-performance state to a comparatively low-performance one, whereas $\tilde{\mu}^{l}_{(i,j)}$ $(i, j = 1, 2, \ldots, k_l, i < j)$ represents the fuzzy number for the corresponding maintenance rate from a low-performance state to the previous high-performance one after appropriate maintenance. In addition, k_l and 1 denote the best and worst FMSC states, and $\tilde{g}_{(l,k_l)}$ denotes the performance fuzzy number of the l^{th} FMSC in state k_l.

FUGF combines UGF and fuzzy membership functions, and it is widely used to determine the dynamic performance of large and complex FMSS configurations [10], thereby facilitating analysis of the transient FMSS dynamic performance. If there exist M FMSCs in a given FMSS with component l containing k_l differently performing states, the performance-state space of component l in the system can be expressed as a fuzzy set $\tilde{\mathbf{g}}_l = \{\tilde{g}_{(l,1)}, \tilde{g}_{(l,2)}, \cdots, \tilde{g}_{(l,k_l)}\}$, and its corresponding ISP can be expressed as a fuzzy set $\tilde{\mathbf{p}}_l(t) = \{\tilde{p}_{(l,1)}(t), \tilde{p}_{(l,2)}(t), \cdots, \tilde{p}_{(l,k_l)}(t)\}$. The notation $\tilde{g}_{(l,i)}$ represents the performance fuzzy number for component l in state i, whereas $\tilde{p}_{(l,i)}(t)$ represents the corresponding ISP fuzzy number at time t with $i \in \{1, 2, \ldots, k_l\}$ and $l \in \{1, \ldots, M\}$. The fuzzy transition-intensity matrix for an FMSC that combines $\tilde{\lambda}^{l}_{(i,j)}$ and $\tilde{\mu}^{l}_{(i,j)}$ can be expressed as $\tilde{\mathbf{A}}^{l} = [\tilde{a}^{l}_{(i,j)}]$, $i, j \in 1, 2, \ldots, k_l$ (Fig. 1). Therefore, the fuzzy Chapman–Kolmogorov equations for an FMSC in a given FMSS can be expressed as

$$\frac{d\tilde{p}_{(l,i)}(t)}{dt} = \left[\sum_{\substack{j=1 \\ j\neq i}}^{k_l} \tilde{p}_{(l,j)}(t)\,\tilde{a}^{l}_{(j,i)}\right] - \tilde{p}_{(l,i)}(t) \sum_{\substack{j=1 \\ j\neq i}}^{k_l} \tilde{a}^{l}_{(i,j)}$$
$$i = \{1, 2, \ldots, k_l\}, l = \{1, \ldots, M\} \quad (1)$$

Considering the FMSC to exist initially in its best-performance state k_l, which means the initial state is given by $\tilde{p}_{(l,k_l)}(0) = 1$ and $\tilde{p}_{(l,i)}(0) = 0 (i \neq k_l)$, the fuzzy ISP $\tilde{p}_{(l,i)}(t)$—a function of the fuzzy state-transition-intensity matrix $\tilde{\mathbf{A}}^{l}$ and time—can be deduced by solving the above fuzzy Chapman–Kolmogorov equations. According to the fuzzy-extension principle [22], [23], the upper and lower bounds $(\tilde{p}^{U}_{(l,i)\alpha}(t) = \max f_{(l,i)}(\mathbf{A}^{l}, t)$ and $\tilde{p}^{L}_{(l,i)\alpha}(t) = \min f_{(l,i)}(\mathbf{A}^{l}, t)$, respectively) of the l^{th} FMSC ISP in the α-cut level interval could be obtained by optimizing the following parameter-planning model.

1. Lower-bound optimization of FMSC parameter-planning model:

$$\begin{aligned}
&\min\ f_{(l,i)}(\mathbf{A}^{l}, t) \quad (t \geq 0, 0 \leq \alpha \leq 1, 1 \leq l \leq M)\\
&s.t.\ \tilde{\lambda}^{l,L}_{(k_l,k_{l-1})\alpha} \leq \lambda^{l}_{(k_l,\,k_{l-1})} \leq \tilde{\lambda}^{l,U}_{(k_l,\,k_{l-1})\alpha}\\
&\quad\vdots\\
&\quad\tilde{\lambda}^{l,L}_{(2,1)\alpha} \leq \lambda^{l}_{(2,1)} \leq \tilde{\lambda}^{l,U}_{(2,1)\alpha}\\
&\quad\tilde{\mu}^{l,L}_{(k_{l-1},k_l)\alpha} \leq \mu^{l}_{(k_{l-1},k_l)} \leq \tilde{\mu}^{l,U}_{(k_{l-1},k_l)\alpha}\\
&\quad\vdots\\
&\quad\tilde{\mu}^{l,L}_{(1,2)\alpha} \leq \mu^{l}_{(1,2)} \leq \tilde{\mu}^{l,U}_{(1,2)\alpha}
\end{aligned} \quad (2)$$

2. Upper-bound optimization of FMSC parameter-planning model:

$$\begin{aligned}
&\max\ f_{(l,i)}(\mathbf{A}^{l}, t) \quad (t \geq 0, 0 \leq \alpha \leq 1, 1 \leq l \leq M)\\
&s.t.\ \tilde{\lambda}^{l,L}_{(k_l,k_{l-1})\alpha} \leq \lambda^{l}_{(k_l,\,k_{l-1})} \leq \tilde{\lambda}^{l,U}_{(k_l,\,k_{l-1})\alpha}\\
&\quad\vdots\\
&\quad\tilde{\lambda}^{l,L}_{(2,1)\alpha} \leq \lambda^{l}_{(2,1)} \leq \tilde{\lambda}^{l,U}_{(2,1)\alpha}\\
&\quad\tilde{\mu}^{l,L}_{(k_{l-1},k_l)\alpha} \leq \mu^{l}_{(k_{l-1},k_l)} \leq \tilde{\mu}^{l,U}_{(k_{l-1},k_l)\alpha}\\
&\quad\vdots\\
&\quad\tilde{\mu}^{l,L}_{(1,2)\alpha} \leq \mu^{l}_{(1,2)} \leq \tilde{\mu}^{l,U}_{(1,2)\alpha}
\end{aligned} \quad (3)$$

The FMSC ISP can then be established in the form of FUGF $\tilde{U}_s(z,t)$ based on the FMSS structure function using operator $\tilde{\Omega}_\phi$ reported in [24] as follows.

$$\begin{aligned}&\tilde{U}_s(z,t)\\&=\tilde{\Omega}_\phi\left[\sum_{i_1=1}^{k_1}\tilde{p}_{(1,i_1)}(t)\cdot z^{\tilde{g}_{(1,i_1)}},\cdots,\sum_{i_M=1}^{k_M}\tilde{p}_{(M,i_M)}(t)\cdot z^{\tilde{g}_{(M,i_M)}}\right]\\&=\sum_{i_1=1}^{k_1}\sum_{i_2=1}^{k_2}\cdots\sum_{i_M=1}^{k_M}\left[\prod_{l=1}^{M}\tilde{p}_{(l,i_l)}(t)\cdot z^{\phi\left(\tilde{g}_{(l,i_1)},\cdots,\tilde{g}_{(M,i_M)}\right)}\right]\\&=\sum_{i=1}^{K_s}\tilde{P}_{(s,i)}(t)\cdot z^{\tilde{g}_{(s,i)}}\end{aligned}\tag{4}$$

Here, M denotes the total number of components constituting the system with state K_s performance and $\phi(\cdot)$ denotes the FMSS structure-function. From equation (4), the FMSS ISP can be expressed as

$$\tilde{P}_{(s,i)}(t)=\prod_{l=1}^{M}\tilde{p}_{(l,i_l)}(t)\tag{5}$$

Similarly, the upper ($\tilde{P}^U_{(s,i)\alpha}(t)$) and lower ($\tilde{P}^L_{(s,i)\alpha}(t)$) bounds representing the FMSS ISP in the α-cut level interval can be deduced by optimizing the following parameter-planning model.

1. Lower-bound optimization of FMSS parameter-planning model:

$$\begin{aligned}\tilde{P}^L_{(s,i)\alpha}(t)=\min&\prod_{l=1}^{M}p_{(l,i_l)}(t),\quad\begin{pmatrix}t\ge 0,0\le\alpha\le 1,\\1\le l\le M\end{pmatrix}\\s.t.\ &\tilde{\lambda}^{l,L}_{(k_l,k_{l-1})\alpha}\le\lambda^{l}_{(k_l,\,k_{l-1})}\le\tilde{\lambda}^{l,U}_{(k_l,\,k_{l-1})\alpha}\\&\vdots\\&\tilde{\lambda}^{l,L}_{(2,1)\alpha}\le\lambda^{l}_{(2,1)}\le\tilde{\lambda}^{l,U}_{(2,1)\alpha}\\&\tilde{\mu}^{l,L}_{(k_{l-1},k_l)\alpha}\le\mu^{l}_{(k_{l-1},k_l)}\le\tilde{\mu}^{l,U}_{(k_{l-1},k_l)\alpha}\\&\vdots\\&\tilde{\mu}^{l,L}_{(1,2)\alpha}\le\mu^{l}_{(1,2)}\le\tilde{\mu}^{l,U}_{(1,2)\alpha}\end{aligned}\tag{6}$$

2. Upper-bound optimization of FMSS parameter-planning model:

$$\begin{aligned}\tilde{P}^U_{(s,i)\alpha}(t)=\max&\prod_{l=1}^{M}p_{(l,i_l)}(t),\quad\begin{pmatrix}t\ge 0,0\le\alpha\le 1,\\1\le l\le M\end{pmatrix}\\s.t.\ &\tilde{\lambda}^{l,L}_{(k_l,k_{l-1})\alpha}\le\lambda^{l}_{(k_l,\,k_{l-1})}\le\tilde{\lambda}^{l,U}_{(k_l,\,k_{l-1})\alpha}\\&\vdots\\&\tilde{\lambda}^{l,L}_{(2,1)\alpha}\le\lambda^{l}_{(2,1)}\le\tilde{\lambda}^{l,U}_{(2,1)\alpha}\\&\tilde{\mu}^{l,L}_{(k_{l-1},k_l)\alpha}\le\mu^{l}_{(k_{l-1},k_l)}\le\tilde{\mu}^{l,U}_{(k_{l-1},k_l)\alpha}\\&\vdots\\&\tilde{\mu}^{l,L}_{(1,2)\alpha}\le\mu^{l}_{(1,2)}\le\tilde{\mu}^{l,U}_{(1,2)\alpha}\end{aligned}\tag{7}$$

The FMSS performance $\tilde{g}_{(s,i)}=\phi\left(\tilde{g}_{(1,i_1)},\cdots,\tilde{g}_{(M,i_M)}\right)$ can be evaluated using the previously obtained FMSC state performance based on the FMSS structure-function by employing a mapping procedure. The $\tilde{g}_{(s,i)}$ value in the α-cut level interval can be obtained using the below expression.

$$\begin{aligned}&\tilde{g}_{(s,i)\alpha}\\&=\begin{bmatrix}\min\phi\left(\tilde{g}_{(1,i_1)},\cdots,\tilde{g}_{(M,\,i_M)};\mu_{\tilde{g}_{(l,i_l)}}(g_{(l,i_l)})\ge\alpha\right),\\\max\phi\left(\tilde{g}_{(1,i_1)},\cdots,\tilde{g}_{(M,i_M)};\mu_{\tilde{g}_{(l,i_l)}}(g_{(l,i_l)})\ge\alpha\right)\end{bmatrix}\\&=\left[\tilde{g}^L_{(s,i)\alpha},\ \tilde{g}^U_{(s,i)\alpha}\right]\qquad(1\le l\le M,0\le\alpha\le 1)\end{aligned}\tag{8}$$

Accordingly, the upper and lower bounds ($\tilde{g}^U_{(s,\,i)\alpha}$ and $\tilde{g}^L_{(s,i)\alpha}$, respectively) of FMSS performance in the α-cut level interval can be obtained by optimizing the following parameter-planning model.

1. Lower-bound optimization of parameter-planning model for FMSS performance:

$$\begin{aligned}\tilde{g}^L_{(s,i)\alpha}=\min&\,\phi\left(\tilde{g}_{(1,i_1)},\ \cdots,\tilde{g}_{(M,i_M)};\mu_{\tilde{g}_{(l,i_l)}}(g_{(l,i_l)})\ge\alpha\right),\\&(0\le\alpha\le 1,1\le l\le M)\\s.t.\ &\tilde{g}^L_{(l,i_1)\alpha}\le g_{(l,i_1)}\le\tilde{g}^U_{(l,i_1)\alpha}\\&\vdots\\&\tilde{g}^L_{(l,i_M)\alpha}\le g_{(l,i_M)}\le\tilde{g}^U_{(l,i_M)\alpha}\end{aligned}\tag{9}$$

2. Upper-bound optimization of parameter-planning model for FMSS performance:

$$\begin{aligned}\tilde{g}^U_{(s,i)\alpha}=\max&\,\phi\left(\tilde{g}_{(1,i_1)},\ \cdots,\tilde{g}_{(M,i_M)};\mu_{\tilde{g}_{(l,i_l)}}(g_{(l,i_l)})\ge\alpha\right),\\&(0\le\alpha\le 1,1\le l\le M)\\s.t.\ &\tilde{g}^L_{(l,i_1)\alpha}\le g_{(l,i_1)}\le\tilde{g}^U_{(l,i_1)\alpha}\\&\vdots\\&\tilde{g}^L_{(l,i_M)\alpha}\le g_{(l,i_M)}\le\tilde{g}^U_{(l,i_M)\alpha}\end{aligned}\tag{10}$$

For a commonly used series–parallel configuration with a flow-transmission system, the FMSS-state performance can be expressed as the following function of the FMSC state performance in the TFN form—$\tilde{g}_{(l,i_l)}\left(a_{(l,i_l)},b_{(l,i_l)},c_{(l,i_l)}\right)(1\le l\le M,1\le i_l\le k_l)$—based on the MSS structure function $\phi(\cdot)$ [10].

1. Parallel system:

$$\begin{aligned}\tilde{g}_{(s,i)}&=\phi_p\left(\tilde{g}_{(1,i_1)},\cdots\,\tilde{g}_{(l,i_l)}\cdots,\,\tilde{g}_{(M,i_M)}\right)\\&=\left(\sum_{l=1}^{M}a_{(l,i_l)},\sum_{l=1}^{M}b_{(l,i_l)},\sum_{l=1}^{M}c_{(l,i_l)}\right)\end{aligned}\tag{11}$$

2. Series system:

$$\begin{aligned}\tilde{g}_{(s,i)}&=\phi_s\left(\tilde{g}_{(1,i_1)},\cdots\,\tilde{g}_{(l,i_l)}\cdots,\,\tilde{g}_{(M,i_M)}\right)\\&=\min\left(\tilde{g}_{(1,i_1)},\cdots\tilde{g}_{(l,i_l)}\cdots,\tilde{g}_{(M,i_M)}\right)\\&=\begin{pmatrix}\min\left(a_{(1,i_1)},\cdots\,a_{(l,i_l)}\cdots,a_{(M,i_M)}\right),\\\min\left(b_{(1,i_1)},\cdots b_{(l,i_l)}\cdots,b_{(M,\,i_M)}\right),\\\min\left(c_{(1,i_1)},\cdots\,c_{(l,i_l)}\cdots,c_{(M,i_M)}\right)\end{pmatrix}\end{aligned}\tag{12}$$

III. IMPROVED FMSS AVAILABILITY INDEX

The FMSS availability index developed in previous studies has two major shortcomings. First, the existing FMSS availability membership function breaches the concept of normal convex sets [11], [12] in fuzzy theory beyond the fuzziness expansion of availability. Second, the said membership function violates the rule of summation over unit probabilities [10]. To address these concerns, this paper presents an improved FMSS availability index that satisfies the fuzzy principle as follows.

(1) The normal convex set principle is adhered to in fuzzy theory.
(2) The improved FMSS availability with α-cut level equal to 1 conforms to the MSS availability of crisp observations.
(3) The summation over state probabilities equals 1 when determining the FMSS availability.

The following steps outline the calculation of the proposed improved FMSS availability index.

Step 1: *Establish the fuzzy Markov stochastic model for FMSCs*

The fuzzy Chapman–Kolmogorov equations (1) for FMSCs in a given FMSS are first established using the fuzzy transition intensities derived from the FMSC state-transition diagram (Fig. 1).

Step 2: Determine fuzzy ISP of FMSCs

The MSS complexity caused by the inclusion of several FMSCs makes it impractical to obtain analytical solutions. To address this concern, the numerical–analytical approaches extensively used across different fields can be used to evaluate fuzzy FMSCs ISP given by $\tilde{p}_{(l,i)\alpha}(t)$ [25].

Step 3: *Establish FUGF for FMSS*

The FMSS FUGF represents the FMSS ISP can be established by substituting the FMSC FUGF as an algebraic calculation (as described in (4)) as

$$\tilde{u}_l(z,t) = \sum_{i=1}^{k_l} \tilde{p}_{(l,i)}(t) z^{\tilde{g}_{(l,i)}}, \quad l = 1, \ldots, M \tag{13}$$

Step 4: Determine FMSS ISP interval and corresponding performance

By establishing the FMSS parameter-planning model using (6) and (7), the lower and upper bounds of $\tilde{P}_{(s,i)\alpha}(t) = [\tilde{P}^L_{(s,i)\alpha}(t),\ \tilde{P}^U_{(s,i)\alpha}(t)]$ can be obtained in the α-cut level interval after completion of the optimization process. Similarly, using (9)–(12), the lower and upper bounds of the FMSS fuzzy-state performance $\tilde{g}_{(s,\,i)\alpha} = [\tilde{g}^L_{(s,i)\alpha},\ \tilde{g}^U_{(s,i)\alpha}]$ in the α-cut level interval can be evaluated via the model establishment and optimization processes.

Step 5: Establish improved FMSS availability index

By constructing a constrained nonlinear parameter-programming model, the lower and upper bounds of the improved FMSS availability index $\tilde{A}_\alpha(t,\tilde{w}) = [\tilde{A}^L_\alpha(t,\tilde{w}), \tilde{A}^U_\alpha(t,\tilde{w})]$ in the α-cut level interval can be obtained as follows.

1. Optimization model for lower-bound parameter planning of improved FMSS availability index:

$$\begin{aligned}
&\tilde{A}^L_\alpha(t,\tilde{w}) \\
&= \min \sum_{i=1}^{K_s} P_{(w,i)\alpha}(t) \cdot |ar_i|^{rel}_\alpha, \quad (t \geq 0, 0 \leq \alpha \leq 1) \\
&\quad s.t.\ \ \tilde{\mu}_{\tilde{A}^L_\alpha}(t,\tilde{w}) = \mu_A(t,w) + m^L \left(\tilde{A}^L_\alpha(t,\tilde{w}) - A(t,w)\right) \\
&\quad \tilde{P}^L_{(s,i)\alpha}(t) \leq P_{(s,i)}(t) \leq \tilde{P}^U_{(s,\,i)\alpha}(t)
\end{aligned} \tag{14}$$

2. Optimization model for upper-bound parameter planning of improved FMSS availability index:

$$\begin{aligned}
&\tilde{A}^U_\alpha(t,\tilde{w}) \\
&= \max \sum_{i=1}^{Ks} P_{(w,i)\alpha}(t) \cdot |ar_i|^{rel}_\alpha, \quad (t \geq 0, 0 \leq \alpha \leq 1) \\
&\quad s.t.\ \ \tilde{\mu}_{\tilde{A}^U_\alpha}(t,\ \tilde{w}) = \mu_A(t,w) + m^U \left(\tilde{A}^U_\alpha(t,\tilde{w}) - A(t,w)\right) \\
&\quad \tilde{P}^L_{(s,i)\alpha}(t) \leq P_{(s,i)}(t) \leq P^U_{(s,i)\alpha}(t)
\end{aligned} \tag{15}$$

The above equations use the relative cardinality $|ar_i|^{rel}_\alpha$ [11] to quantify the extent to which the FMSS performance fulfills the mission demand. $\tilde{\mu}_{\tilde{A}^L_\alpha}(t,\tilde{w})$ and $\tilde{\mu}_{\tilde{A}^U_\alpha}(t,\ \tilde{w})$ denote the membership functions for $\tilde{A}^L_\alpha(t,\tilde{w})$ and $\tilde{A}^U_\alpha(t,\ \tilde{w})$,respectively. $A(t,w)$ is the crisp value of availability, and $\mu_A(t,w)$ is the corresponding membership function. Notably, the expression $P_{(w,i)\alpha}(t) = P_{(s,i)\alpha}(t) \Big/ \sum_{i=1}^{K_s} P_{(s,i)\alpha}(t)$ in the objective function represents a normalized probability responsible for unit FMSS probabilities over states in the FMSS availability calculation.

In addition, the linear constraint confines the feasible solution area in a triangular compass with slopes m^L and m^U, thereby satisfying the KKT condition [21]. Thus, through an optimization process, the improved FMSS availability index features a linear TFN in compliance with the normal convex set principle in the fuzzy theory. It is noteworthy that TFNs are extensively used for measuring fuzziness in many applications owing to their intuitive and simple algebraic-operation characteristics [26].

IV. ILLUSTRATIVE EXAMPLE

The construction of smart grids has attracted increased attention globally to harness green technologies for cost-effective power generation and more importantly, reduce the harmful effects of greenhouse-gas emissions. Japan's efforts in the construction of smart grids began with the Yokohama Smart City Project (YSCP). A tailor-made smart-grid system that considers specific local environmental features not only utilizes natural resources but also offers further insights into the applications of green technology. A smart grid normally features multiple power performances with non-probabilistic uncertainties related to natural resources mainly owing to geographic reasons. This study focused on a community-based smart grid that combines renewable resources including solar and wind energy with diesel generators, which are traditional power generation sources, into a repairable smart-grid system.

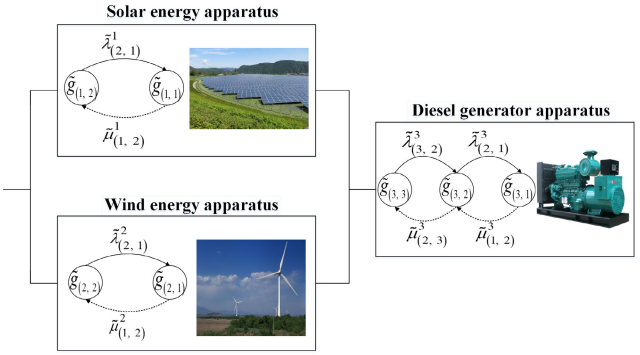

FIGURE 2. FMSS configuration for community-based smart grid.

TABLE 1. TFN for Fuzzy Transition Intensities (Per Year).

Apparatuses	TFN	
Solar energy	$\tilde{\lambda}^1_{(2,1)} = (0.04, 0.05, 0.06)$ $\tilde{\mu}^1_{(1,2)} = (0.4, 0.5, 0.6)$	—
Wind energy	$\tilde{\lambda}^2_{(2,1)} = (0.03, 0.04, 0.05)$ $\tilde{\mu}^2_{(1,2)} = (0.25, 0.3, 0.35)$	—
Diesel generator	$\tilde{\lambda}^3_{(3,2)} = (0.02, 0.03, 0.04)$ $\tilde{\mu}^3_{(2,3)} = (0.2, 0.3, 0.4)$	$\tilde{\lambda}^3_{(2,1)} = (0.01, 0.02, 0.03)$ $\tilde{\mu}^3_{(1,2)} = (0.15, 0.2, 0.25)$

Fig. 2 depicts the system configuration. Wind energy is one of the fastest-growing renewable-energy resources, and it has become an essential alternative to conventional means of electricity generation [27]. However, renewable energy is prone to uncertainties due to environmental changes, and the development cycle of smart grids tends to shorten in some cases. This may lead to non-probabilistic uncertainties when performing reliability-related observations. Therefore, it could be considered appropriate to use the fuzzy multi-state modeling theory compared to the conventional crisp approach to deal with such circumstances. Fig. 2 depicts the two green renewable-energy apparatuses to be connected in parallel and their combination to be serially connected with diesel generators. In accordance with the proposed approach, each energy-resource apparatus serves as an FMSC, thereby constituting the community-based smart-grid FMSS. In this analysis, TFNs were employed without loss of generation to measure the fuzzy transition intensities and evaluate fuzzy performance. Table 1 lists transition-intensity parameters covering both the degradation and maintenance rates while Table 2 lists TFN values for fuzzy power performance. The TFN parameter for power demand was set to 1.9, 2.1, and 2.3 ($\times 10^3$ kW) for the solar-energy, wind-energy, and diesel-generator apparatuses.

Based on the proposed approach, improved FMSS availability can be calculated in the following five steps.

Step 1: Establish fuzzy Markov stochastic model for FMSCs

Substituting the TFN transition intensities (Table 1) corresponding to each energy resource with degradation and maintenance rates in (1) establishes the fuzzy Chapman–Kolmogorov equations pertaining to the three FMSCs based on their respective configurations as follows.

TABLE 2. TFN for Fuzzy Performance ($\times 10^3$) kW.

Apparatuses	State 1	State 2	State 3
Solar energy	0	(1.5, 1.6, 1.7)	—
Wind energy	0	(1.8, 2.0, 2.2)	—
Diesel generator	0	(2.1, 2.4, 2.7)	(3.6, 3.7, 3.8)

FMSC 1: Solar-energy apparatus

$$\begin{cases} \dfrac{d\tilde{p}_{(1,1)}(t)}{dt} = -\tilde{\mu}^1_{(1,2)}\tilde{p}_{(1,1)}(t) + \tilde{\lambda}^1_{(2,1)}\tilde{p}_{(1,2)}(t), \\ \dfrac{d\tilde{p}_{(1,2)}(t)}{dt} = \tilde{\mu}^1_{(1,2)}\tilde{p}_{(1,1)}(t) - \tilde{\lambda}^1_{(2,1)}\tilde{p}_{(1,2)}(t), \end{cases} \quad t \geq 0 \tag{16}$$

FMSC 2: Wind-energy apparatus

$$\begin{cases} \dfrac{d\tilde{p}_{(2,1)}(t)}{dt} = -\tilde{\mu}^2_{(1,2)}\tilde{p}_{(2,1)}(t) + \tilde{\lambda}^2_{(2,1)}\tilde{p}_{(2,2)}(t), \\ \dfrac{d\tilde{p}_{(2,2)}(t)}{dt} = \tilde{\mu}^2_{(1,2)}\tilde{p}_{(2,1)}(t) - \tilde{\lambda}^2_{(2,1)}\tilde{p}_{(2,2)}(t), \end{cases} \quad t \geq 0 \tag{17}$$

FMSC 3: Diesel-generator apparatus

$$\begin{cases} \dfrac{d\tilde{p}_{(3,1)}(t)}{dt} = -\tilde{\mu}^3_{(1,2)}\tilde{p}_{(3,1)}(t) + \tilde{\lambda}^3_{(2,1)}\tilde{p}_{(3,2)}(t), \\ \dfrac{d\tilde{p}_{(3,2)}(t)}{dt} = \tilde{\mu}^3_{(1,2)}\tilde{p}_{(3,1)}(t) - \left(\tilde{\lambda}^3_{(2,1)} + \tilde{\mu}^3_{(2,3)}\right)\tilde{p}_{(3,2)}(t) \\ \qquad + \tilde{\lambda}^3_{(3,2)}\tilde{p}_{(3,3)}(t), \\ \dfrac{d\tilde{p}_{(3,3)}(t)}{dt} = \tilde{\mu}^3_{(2,3)}\tilde{p}_{(3,2)}(t) - \tilde{\lambda}^3_{(3,2)}\tilde{p}_{(3,3)}(t), \end{cases} \quad t \geq 0 \tag{18}$$

The best initial states for all FMSCs are assigned a probability of 1 while other states are assigned zero probability.

Step 2: Determine fuzzy FMSC ISP

Using a numerical–analytical approach, the FMSC ISP can be obtained by solving the simultaneous differential equations established in *Step 1*. Further, the lower and upper ISP bounds could be determined by establishing and optimizing the parameter-planning models pertaining to the solar-energy, wind-energy, and diesel-generator apparatuses using (2) and (3).

Step 3: Establish FMSC FUGF and FMSS ISP

The FMSC ISPs for the solar-energy, wind-energy, and diesel-generator apparatuses can be expressed in the FUGF form as follows.

FMSC 1: Solar-energy apparatus

$$\begin{aligned} \tilde{u}_1(z,t) &= \tilde{p}_{(1,2)}(t)z^{\tilde{g}_{(1,2)}} + \tilde{p}_{(1,1)}(t)z^{\tilde{g}_{(1,1)}} \\ &= \tilde{p}_{(1,2)}(t)z^{(1.5,\ 1.6,1.7)} + \tilde{p}_{(1,1)}(t)z^0 \end{aligned} \tag{19}$$

FMSC 2: Wind-energy apparatus

$$\begin{aligned} \tilde{u}_2(z,t) &= \tilde{p}_{(2,2)}(t)z^{\tilde{g}_{(2,2)}} + \tilde{p}_{(2,1)}(t)z^{\tilde{g}_{(2,1)}} \\ &= \tilde{p}_{(2,2)}(t)z^{(1.8,\ 2.0,2.2)} + \tilde{p}_{(2,1)}(t)z^0 \end{aligned} \tag{20}$$

FMSC 3: Diesel-generator apparatus

$$\begin{aligned}\tilde{u}_3(z,t) &= \tilde{p}_{(3,3)}(t)z^{\tilde{g}_{(3,3)}} + \tilde{p}_{(3,2)}(t)z^{\tilde{g}_{(3,2)}} + \tilde{p}_{(3,1)}(t)z^{\tilde{g}_{(3,1)}} \\ &= \tilde{p}_{(3,3)}(t)z^{(3.6,\ 3.7,3.8)} + \tilde{p}_{(3,2)}(t)z^{(2.1,2.4,2.7)} \\ &\quad + \tilde{p}_{(3,1)}(t)z^{0} \end{aligned} \tag{21}$$

Subsequently, the FMSS ISP for the entire community-based smart grid can be expressed in the FUGF form by using an integration operator and substituting the FUGF of the three FMSCs as follows.

$$\tilde{U}_s(z,t) = \tilde{\Omega}_{\phi}^{ser}\left(\tilde{\Omega}_{\phi}^{par}\left(\tilde{u}_1(z,\ t), \tilde{u}_2(z,t)\right),\ \tilde{u}_3(z,t)\right) \tag{22}$$

Here, $\tilde{\Omega}_{\phi}^{ser}$ and $\tilde{\Omega}_{\phi}^{par}$ denote integration operators for the series and parallel configurations, respectively. The below expression (23) elucidates the integration process for the solar-energy apparatus with the wind-energy apparatus connected in parallel.

$$\begin{aligned}\tilde{\Omega}_{\phi}^{par}\left(\tilde{u}_1(z,\ t), \tilde{u}_2(z,t)\right) &= \tilde{p}_{(1,2)}(t)\tilde{p}_{(2,2)}(t)z^{(3.3,3.6,3.9)} \\ &\quad + \tilde{p}_{(1,1)}(t)\tilde{p}_{(2,2)}(t)z^{(1.8,2.0,2.2)} \\ &\quad + \tilde{p}_{(1,2)}(t)\tilde{p}_{(2,1)}(t)z^{(1.5,1.6,1.7)} \\ &\quad + \tilde{p}_{(1,1)}(t)\tilde{p}_{(2,1)}(t)z^{0} \end{aligned} \tag{23}$$

Likewise, the integration of the above combination connected in series with the diesel-generator apparatus can be performed as described in (24) below.

$$\begin{aligned}\tilde{U}_s(z,t) &= \tilde{\Omega}_{\phi}^{ser}\left(\tilde{\Omega}_{\phi}^{par}\left(\tilde{u}_1(z,\ t), \tilde{u}_2(z,t)\right),\ \tilde{u}_3(z,t)\right) \\ &= \tilde{p}_{(1,1)}(t)\tilde{p}_{(2,1)}(t)\tilde{p}_{(3,1)}(t)z^{(0)} \\ &\quad + \tilde{p}_{(1,1)}(t)\tilde{p}_{(2,1)}(t)\tilde{p}_{(3,2)}(t)z^{(0)} \\ &\quad + \tilde{p}_{(1,1)}(t)\tilde{p}_{(2,1)}(t)\tilde{p}_{(3,3)}(t)z^{(0)} \\ &\quad + \tilde{p}_{(1,1)}(t)\tilde{p}_{(2,2)}(t)\tilde{p}_{(3,1)}(t)z^{(0)} \\ &\quad + \tilde{p}_{(1,1)}(t)\tilde{p}_{(2,2)}(t)\tilde{p}_{(3,2)}(t)z^{(1.8,2.0,2.2)} \\ &\quad + \tilde{p}_{(1,1)}(t)\tilde{p}_{(2,2)}(t)\tilde{p}_{(3,3)}(t)z^{(1.8,2.0,2.2)} \\ &\quad + \tilde{p}_{(1,2)}(t)\tilde{p}_{(2,1)}(t)\tilde{p}_{(3,1)}(t)z^{(0)} \\ &\quad + \tilde{p}_{(1,2)}(t)\tilde{p}_{(2,1)}(t)\tilde{p}_{(3,2)}(t)z^{(1.5,1.6,1.7)} \\ &\quad + \tilde{p}_{(1,2)}(t)\tilde{p}_{(2,1)}(t)\tilde{p}_{(3,3)}(t)z^{(1.5,1.6,1.7)} \\ &\quad + \tilde{p}_{(1,2)}(t)\tilde{p}_{(2,2)}(t)\tilde{p}_{(3,1)}(t)z^{(0)} \\ &\quad + \tilde{p}_{(1,2)}(t)\tilde{p}_{(2,2)}(t)\tilde{p}_{(3,2)}(t)z^{(2.1,2.4,2.7)} \\ &\quad + \tilde{p}_{(1,2)}(t)\tilde{p}_{(2,2)}(t)\tilde{p}_{(3,3)}(t)z^{(3.3,3.6,3.8)} \end{aligned} \tag{24}$$

By extracting the FMSS ISP in the above FUGF form, five distinguished five-state performances of the entire community-based smart grid can be expressed as functions of the FMSC ISPs as described below.

State 1: $\tilde{g}_{(s,1)} = 0$

$$\begin{aligned}\tilde{P}_{(s,1)} &= \tilde{p}_{(1,1)}(t)\tilde{p}_{(2,1)}(t)\tilde{p}_{(3,1)}(t)z^{(0)} \\ &\quad + \tilde{p}_{(1,1)}(t)\tilde{p}_{(2,1)}(t)\tilde{p}_{(3,2)}(t)z^{(0)} \\ &\quad + \tilde{p}_{(1,1)}(t)\tilde{p}_{(2,1)}(t)\tilde{p}_{(3,3)}(t)z^{(0)} \\ &\quad + \tilde{p}_{(1,1)}(t)\tilde{p}_{(2,2)}(t)\tilde{p}_{(3,1)}(t)z^{(0)} \\ &\quad + \tilde{p}_{(1,2)}(t)\tilde{p}_{(2,1)}(t)\tilde{p}_{(3,1)}(t)z^{(0)} \\ &\quad + \tilde{p}_{(1,2)}(t)\tilde{p}_{(2,2)}(t)\tilde{p}_{(3,1)}(t)z^{(0)} \end{aligned} \tag{25}$$

State 2: $\tilde{g}_{(s,2)} = (1.5,\ 1.6,\ 1.7)$

$$\begin{aligned}\tilde{P}_{(s,2)} &= \tilde{p}_{(1,2)}(t)\tilde{p}_{(2,1)}(t)\tilde{p}_{(3,2)}(t)z^{(1.5,1.6,1.7)} \\ &\quad + \tilde{p}_{(1,2)}(t)\tilde{p}_{(2,1)}(t)\tilde{p}_{(3,3)}(t)z^{(1.5,1.6,\ 1.7)} \end{aligned} \tag{26}$$

State 3: $\tilde{g}_{(s,3)} = (1.8,\ 2.0,\ 2.2)$

$$\begin{aligned}\tilde{P}_{(s,3)} &= \tilde{p}_{(1,1)}(t)\tilde{p}_{(2,2)}(t)\tilde{p}_{(3,2)}(t)z^{(1.8,2.0,2.2)} \\ &\quad + \tilde{p}_{(1,1)}(t)\tilde{p}_{(2,2)}(t)\tilde{p}_{(3,3)}(t)z^{(1.8,2.0,\ 2.2)} \end{aligned} \tag{27}$$

State 4: $\tilde{g}_{(s,4)} = (2.1,\ 2.4,\ 2.7)$

$$\tilde{P}_{(s,4)} = \tilde{p}_{(1,2)}(t)\tilde{p}_{(2,2)}(t)\tilde{p}_{(3,2)}(t)z^{(2.1,2.4,2.7)} \tag{28}$$

State 5: $\tilde{g}_{(s,5)} = (3.3,\ 3.6,\ 3.8)$

$$\tilde{P}_{(s,5)} = \tilde{p}_{(1,2)}(t)\tilde{p}_{(2,2)}(t)\tilde{p}_{(3,3)}(t)z^{(3.3,3.6,3.8)} \tag{29}$$

Step 4: Evaluate FMSS ISP interval and corresponding performance

The upper and lower bounds of the five-state FMSS ISP $\tilde{P}_{(s,i)\alpha}(t) = [\tilde{P}^{L}_{(s,\ i)\alpha}(t), \tilde{P}^{U}_{(s,i)\alpha}(t)]$ and corresponding performance $\tilde{g}_{(s,i)\alpha} = [\tilde{g}^{L}_{(s,i)\alpha},\ \tilde{g}^{U}_{(s,i)\alpha}]$ in the α-cut level set can be evaluated post construction and optimization of the parameter-planning models using (6), (7), (9), and (10) as follows.

1. Lower-bound optimization of FMSS parameters-planning model:

$$\begin{aligned}&\tilde{P}^{L}_{(s,i)\alpha}(t) \\ &= \min \prod_{l=1}^{3} p_{(l,i_l)}(t), \quad \begin{pmatrix} t \geq 0, 0 \leq \alpha \leq 1, \\ 1 \leq i \leq 5, 1 \leq i_1 \leq 2, \\ 1 \leq i_2 \leq 2, 1 \leq i_3 \leq 3 \end{pmatrix} \\ &\quad s.t.\ \ \tilde{\lambda}^{1,L}_{(2,1)\alpha} \leq \lambda^{1}_{(2,1)} \leq \tilde{\lambda}^{1,U}_{(2,1)\alpha}, \tilde{\mu}^{1,L}_{(1,2)\alpha} \leq \mu^{1}_{(1,2)} \leq \tilde{\mu}^{1,U}_{(1,2)\alpha} \\ &\qquad \tilde{\lambda}^{2,L}_{(2,1)\alpha} \leq \lambda^{2}_{(2,1)} \leq \tilde{\lambda}^{2,U}_{(2,1)\alpha}, \tilde{\mu}^{2,L}_{(1,2)\alpha} \leq \mu^{2}_{(1,2)} \leq \tilde{\mu}^{2,U}_{(1,2)\alpha} \\ &\qquad \tilde{\lambda}^{3,L}_{(3,2)\alpha} \leq \lambda^{3}_{(3,2)} \leq \tilde{\lambda}^{3,U}_{(3,\ 2)\alpha}, \tilde{\mu}^{3,L}_{(2,3)\alpha} \leq \mu^{3}_{(2,3)} \leq \tilde{\mu}^{3,U}_{(2,3)\alpha} \\ &\qquad \tilde{\lambda}^{3,L}_{(2,1)\alpha} \leq \lambda^{3}_{(2,1)} \leq \tilde{\lambda}^{3,U}_{(2,1)\alpha}, \tilde{\mu}^{3,L}_{(1,2)\alpha} \leq \mu^{3}_{(1,2)} \leq \tilde{\mu}^{3,U}_{(1,2)\alpha} \end{aligned} \tag{30}$$

$$\begin{aligned}&\tilde{g}^{L}_{(s,i)\alpha} \\ &= \min \phi\left(\tilde{g}_{(l,i_l)};\ \mu_{\tilde{g}_{(l,i_l)}}(g_{(l,i_l)}) \geq \alpha\right), \\ &\qquad \begin{pmatrix} 0 \leq \alpha \leq 1, 1 \leq i \leq 5 \\ 1 \leq l \leq 3, 1 \leq i_1 \leq 2 \\ 1 \leq i_2 \leq 2, 1 \leq i_3 \leq 3 \end{pmatrix} \\ &\quad s.t.\ \ \tilde{g}^{L}_{(l,i_l)\alpha} \leq g_{(l,i_l)} \leq \tilde{g}^{U}_{(l,i_l)\alpha} \end{aligned} \tag{31}$$

2. Upper-bound optimization of FMSS parameters-planning model:

$$\begin{aligned}&\tilde{P}^{U}_{(s,i)\alpha}(t) \\ &= \max \prod_{l=1}^{3} p_{(l,i_l)}(t), \begin{pmatrix} t \geq 0, 0 \leq \alpha \leq 1, \\ 1 \leq i \leq 5, 1 \leq i_1 \leq 2, \\ 1 \leq i_2 \leq 2, 1 \leq i_3 \leq 3 \end{pmatrix} \\ &\quad s.t.\ \ \tilde{\lambda}^{1,L}_{(2,1)\alpha} \leq \lambda^{1}_{(2,1)} \leq \tilde{\lambda}^{1,U}_{(2,1)\alpha}, \tilde{\mu}^{1,L}_{(1,2)\alpha} \leq \mu^{1}_{(1,2)} \leq \tilde{\mu}^{1,U}_{(1,2)\alpha} \\ &\qquad \tilde{\lambda}^{2,L}_{(2,1)\alpha} \leq \lambda^{2}_{(2,1)} \leq \tilde{\lambda}^{2,U}_{(2,1)\alpha}, \tilde{\mu}^{2,L}_{(1,2)\alpha} \leq \mu^{2}_{(1,2)} \leq \tilde{\mu}^{2,U}_{(1,2)\alpha} \\ &\qquad \tilde{\lambda}^{3,L}_{(3,2)\alpha} \leq \lambda^{3}_{(3,2)} \leq \tilde{\lambda}^{3,U}_{(3,2)\alpha}, \tilde{\mu}^{3,L}_{(2,3)\alpha} \leq \mu^{3}_{(2,3)} \leq \tilde{\mu}^{3,U}_{(2,3)\alpha} \\ &\qquad \tilde{\lambda}^{3,L}_{(2,1)\alpha} \leq \lambda^{3}_{(2,1)} \leq \tilde{\lambda}^{3,U}_{(2,1)\alpha}, \tilde{\mu}^{3,L}_{(1,2)\alpha} \leq \mu^{3}_{(1,2)} \leq \tilde{\mu}^{3,U}_{(1,2)\alpha} \end{aligned} \tag{32}$$

$$\tilde{g}^{U}_{(s,i)\alpha} = \max \phi\left(\tilde{g}_{(l,i_l)};\ \mu_{\tilde{g}_{(l,i_l)}}(g_{(l,i_l)}) \geq \alpha\right), \begin{pmatrix} 0 \leq \alpha \leq 1, 1 \leq i \leq 5 \\ 1 \leq l \leq 3, 1 \leq i_1 \leq 2 \\ 1 \leq i_2 \leq 2, 1 \leq i_3 \leq 3 \end{pmatrix}$$
$$s.t.\ \ \tilde{g}^{L}_{(l,i_l)\alpha} \leq g_{(l,i_l)} \leq \tilde{g}^{U}_{(l,i_l)\alpha} \quad (33)$$

Thus, based on the calculations performed in this step, a three-dimensional plot can be generated to depict the ISP of the entire community-based smart grid with a mission time of 60 years and membership values plotted on the x and y axes, respectively. Figs. 3–7 depict the said three-dimensional diagrams for FMSS ISPs for the said five states. As can be seen in the figures, for α-cut $= 1$, the individual state ISPs converge to a single-point time-varying probability, thereby representing a crisp circumstance indicated by the red line. This three-dimensional ISP patterns offer further insight into not only the time-varying ISP trajectory but also the impact of circumstance fussiness on ISP beyond the mission-time and fuzziness interactions. The said plot facilitates engineer to conceive a more cost-effective upgrade to existing smart grids as well as improve maintenance strategies.

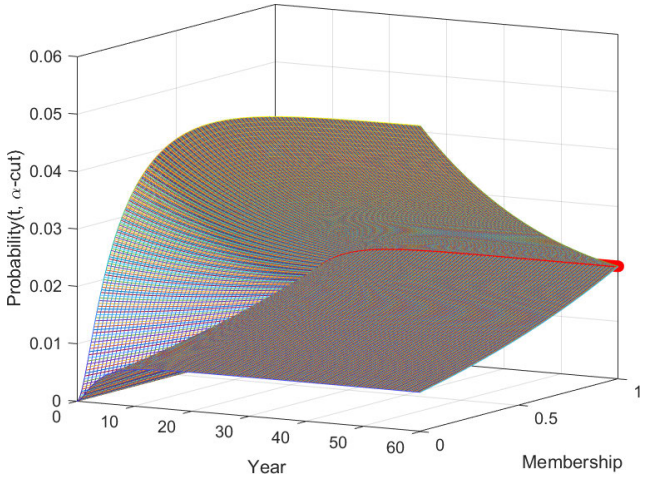

FIGURE 3. Three-dimensional FMSS ISP plot for State 1.

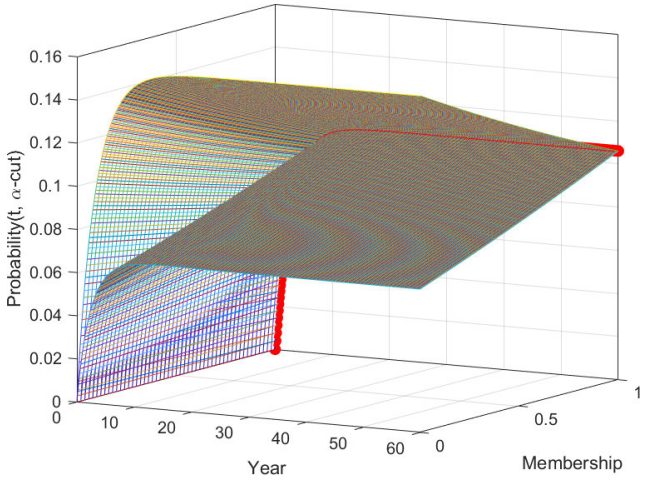

FIGURE 4. Three-dimensional FMSS ISP plot for State 2.

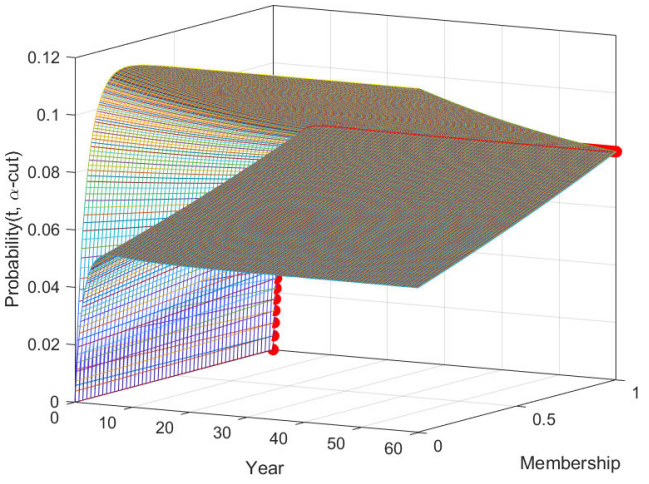

FIGURE 5. Three-dimensional FMSS ISP plot for State 3.

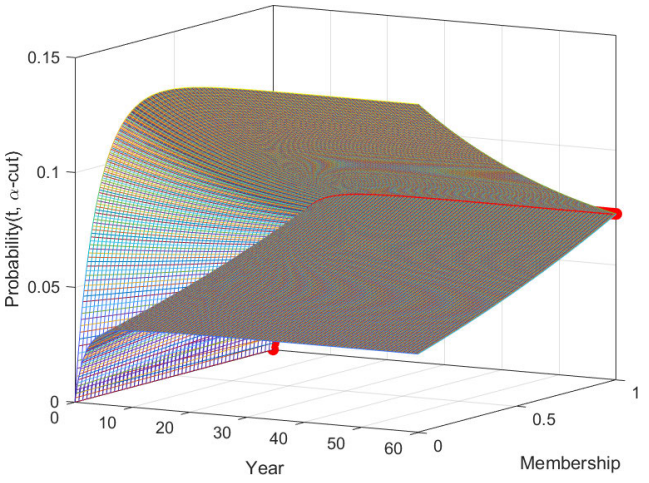

FIGURE 6. Three-dimensional FMSS ISP plot for State 4.

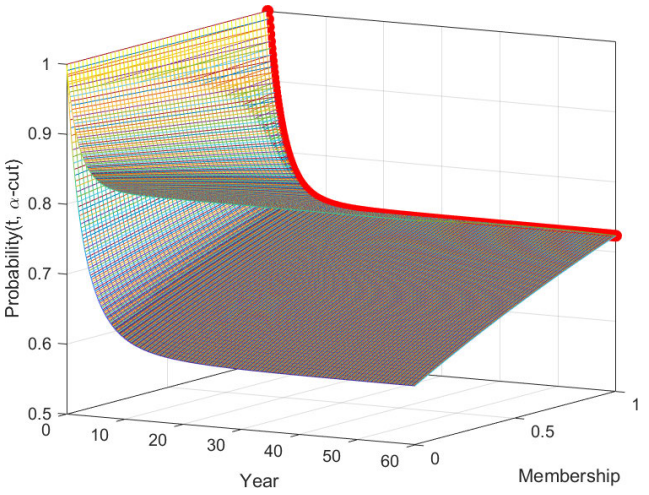

FIGURE 7. Three-dimensional FMSS ISP plot for State 5.

Step 5: Establish improved FMSS availability index

Given a target power demand of $\tilde{w} = (1.9, 2.1, 2.3) \times 10^3$ kW, the lower and upper bounds of the improved FMSS availability in the α-cut level set for the community-based

TABLE 3. FMSS steady-state availability in a-cut level set.

α-cut	Approach by Liu *et al.* [11]	Proposed approach
	$\left[\tilde{A}_{\alpha}^{L}(t,\tilde{w}),\tilde{A}_{\alpha}^{U}(t,\tilde{w})\right]$	$\left[\tilde{A}_{\alpha}^{L}(t,\tilde{w}),\tilde{A}_{\alpha}^{U}(t,\tilde{w})\right]$
0.0	[0.6977, 0.8861]	[0.6969, 0.8888]
0.1	[0.7116, 0.8800]	[0.7067, 0.8794]
0.2	[0.7244, 0.8735]	[0.7165, 0.8700]
0.3	[0.7359, 0.8662]	[0.7263, 0.8606]
0.4	[0.7453, 0.8576]	[0.7361, 0.8512]
0.5	[0.7526, 0.8472]	[0.7459, 0.8419]
0.6	[0.7589, 0.8357]	[0.7557, 0.8325]
0.7	[0.7649, 0.8235]	[0.7655, 0.8231]
0.8	[0.7745, 0.8137]	[0.7753, 0.8137]
0.9	[0.7849, 0.8045]	[0.7851, 0.8043]
1.0	[0.7949, 0.7949]	[0.7949, 0.7949]

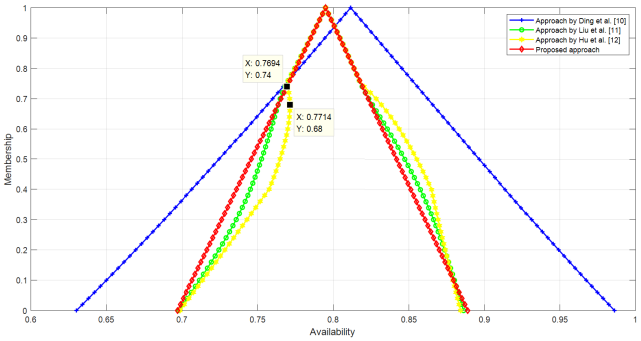

FIGURE 8. Comparison between steady-state FMSS availabilities obtained using proposed approach and those presented in [10]–[12].

smart grid can be obtained using the proposed constrained nonlinear parameter-planning model equations (14) and (15). As observed in this case study, the performances of states 3 and 4 overlap with the target power demand, i.e., $\tilde{g}_{(s,\,3)} \leq \tilde{w}$ and $\tilde{g}_{(s,4)} \geq \tilde{w}$. Table 3 compares the results obtained in this study against those obtained using the method reported in [11]. Fig. 8 presents a comparison between steady-state availability results obtained using the proposed method against those reported in [10]–[12]. As can be observed, the proposed improved FMSS availability for α-cut=1 converges to a crisp value of 0.7949. For the general MSS considered in this case with no fuzziness, the crisp values of the performance of states 1–5 equaled 0, 1.6, 2, 2.4, and $3.6(\times 10^3 kW)$, respectively. The corresponding MSS availability can be calculated via probability summation over states 4 and 5 that fulfill the power demand of $\tilde{w} = 2.1$ kW. As observed, the result of the calculation coincides with the proposed FMSS convergence value of 0.7949. Notably, the methods reported in [11] and [12] feature a nonlinear trajectory in Fig. 8 despite compliance with the general MSS availability for a crisp circumstance. For example, the calculation performed in accordance with [12] reveals that the lower bound of FMSS availability reduces from 0.7714 to 0.7694 with an increase in the α-cut level set in the 0.68–0.74 interval. This tendency violates the normal convex set principle in the fuzzy theory.

As an added advantage, the three-dimensional plot (Fig. 9) of the improved FMSS availability reveals a further insight

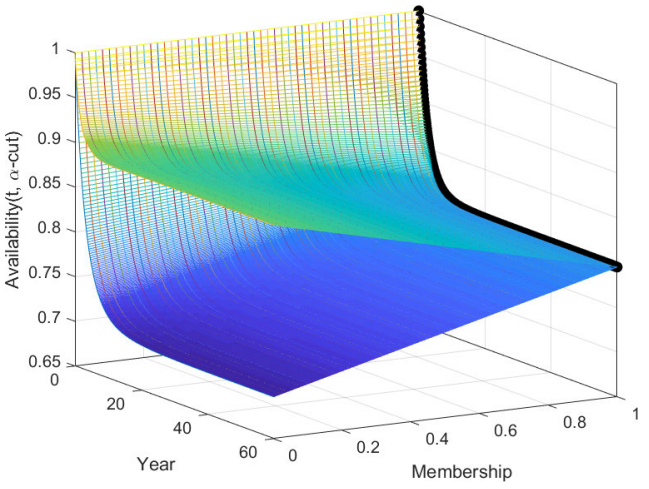

FIGURE 9. Improved FMSS availability with time and membership.

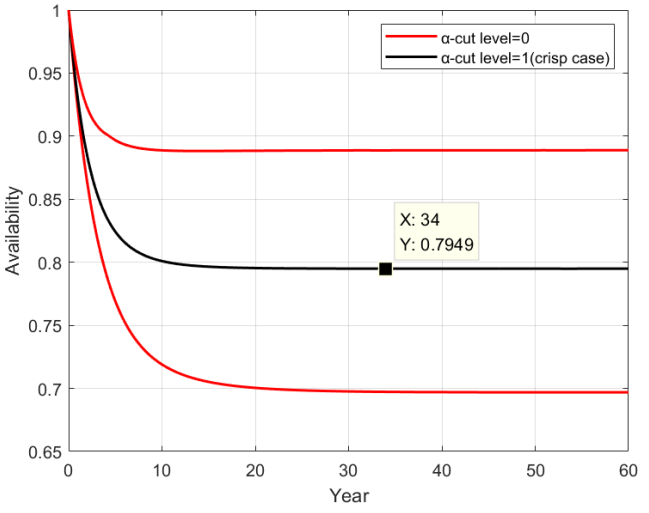

FIGURE 10. The improved FMSS availabilities for α-cut = 0 and 1.

in the efficacy and power capacity of the community-based grid structure related to time and membership. As can be seen, the black line depicts a tendency of a crisp circumstance with α-cut=1. Fig. 10 compares the corresponding FMSS availabilities for α-cut = 0 and 1, respectively. From Fig. 10, it can be inferred that the availability initially reduces with time attaining a steady-state after approximately 34 years, given α-cut = 1.

V. SENSITIVITY ANALYSIS

By verifying the proposed approach beyond looking into the robustness of mathematical models, sensitivity analyses were performed in this study for three exclusive scenarios. In the first scenario, the degradation and maintenance rates were applied with scale-factor values of 0.9 and 1.1, respectively. Subsequently, these scale-values for the said rates were swapped, thereby simulating better and worse circumstances compared to the current case settings with both factors set to 1. In the second scenario, scale factors of 0.8 and 1.2 were applied to the fuzziness of the maintenance rate to simulate

TABLE 4. Altered parameter settings to simulate better and worse circumstances of degradation and maintenance rates.

Worse circumstance $\lambda\times1.1$ and $\mu\times0.9$	Better circumstance $\lambda\times0.9$ and $\mu\times1.1$
Solar energy:	Solar energy:
$\tilde{\lambda}^1_{(2,\,1)}=(0.044,\ 0.055,\ 0.066)$	$\tilde{\lambda}^1_{(2,\,1)}=(0.036,\ 0.045,\ 0.054)$
$\tilde{\mu}^1_{(1,\,2)}=(0.36,\ 0.45,\ 0.54)$	$\tilde{\mu}^1_{(1,\,2)}=(0.44,\ 0.55,\ 0.66)$
Wind energy:	Wind energy:
$\tilde{\lambda}^2_{(2,\,1)}=(0.033,\ 0.044,\ 0.055)$	$\tilde{\lambda}^2_{(2,\,1)}=(0.027,\ 0.036,\ 0.045)$
$\tilde{\mu}^2_{(1,\,2)}=(0.225,\ 0.27,\ 0.315)$	$\tilde{\mu}^2_{(1,\,2)}=(0.275,\ 0.33,\ 0.385)$
Diesel generator:	Diesel generator:
$\tilde{\lambda}^3_{(2,\,1)}=(0.011,\ 0.022,\ 0.033)$	$\tilde{\lambda}^3_{(2,\,1)}=(0.009,\ 0.018,\ 0.027)$
$\tilde{\lambda}^3_{(3,\,2)}=(0.022,\ 0.033,\ 0.044)$	$\tilde{\lambda}^3_{(3,\,2)}=(0.018,\ 0.027,\ 0.036)$
$\tilde{\mu}^3_{(1,\,2)}=(0.165,\ 0.22,\ 0.275)$	$\tilde{\mu}^3_{(1,\,2)}=(0.165,\ 0.22,\ 0.275)$
$\tilde{\mu}^3_{(2,\,3)}=(0.18,\ 0.27,\ 0.36)$	$\tilde{\mu}^3_{(2,\,3)}=(0.22,\ 0.33,\ 0.44)$

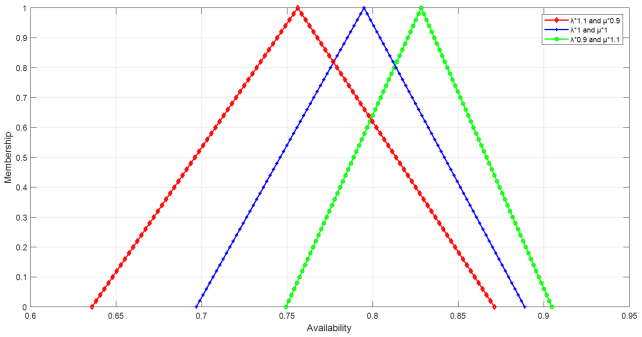

FIGURE 11. Improved steady-state FMSS availability considered altered degradation and maintenance rates of entire smart-grid system.

the expansion and contraction of the FMSS fuzziness. Finally, given the essential role played by the diesel-generator apparatus in the series–parallel configuration of smart-grid systems, scale factors of 0.9 and 1.1 applied to the corresponding degradation and maintenance rates, followed by subsequent swapping, to simulate the better and worse circumstance compared to the current case.

A. SENSITIVITY TO DEGRADATION AND MAINTENANCE RATES OF ENTIRE SMART GRID

Table 4 presents a comparison between the better and worse circumstances obtained via the application of the above-defined scale factors to solar-energy, wind-energy, and diesel-generator apparatuses of the smart-grid system. The corresponding FMSS steady-state availability diagram is depicted in Fig. 11. As anticipated, the better circumstance (green trend) outperforms the worse circumstance (red trend) in terms of the FMSS availability over a smaller α-cut level set interval. The FMSS availability of the original setting (blue trend) falls between the red and green trends. This verifies the accuracy and effectiveness of the proposed approach.

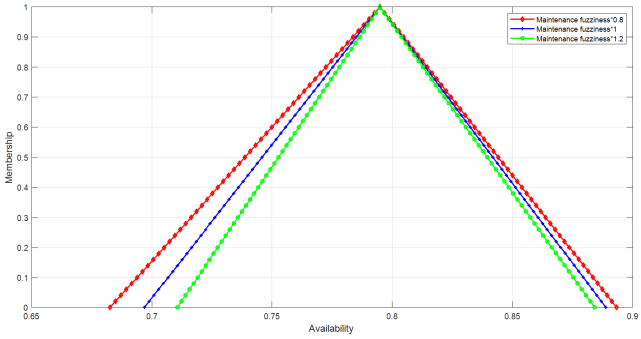

FIGURE 12. Improved steady-state FMSS availability considering altered maintenance fuzziness.

TABLE 5. TFN parameters settings for alteration of maintenance fuzziness.

Worse circumstance Maintenance fuzziness*1.2	Better circumstance Maintenance fuzziness*0.8
Solar energy:	Solar energy:
$\tilde{\mu}^1_{(1,\,2)}=(0.38,\ 0.5,\ 0.62)$	$\tilde{\mu}^1_{(1,\,2)}=(0.42,\ 0.5,\ 0.58)$
Wind energy:	Wind energy:
$\tilde{\mu}^2_{(1,\,2)}=(0.24,\ 0.3,\ 0.36)$	$\tilde{\mu}^2_{(1,\,2)}=(0.26,\ 0.3,\ 0.34)$
Diesel generator:	Diesel generator:
$\tilde{\mu}^3_{(2,\,3)}=(0.18,\ 0.3,\ 0.42)$	$\tilde{\mu}^3_{(2,\,3)}=(0.22,\ 0.3,\ 0.38)$
$\tilde{\mu}^3_{(1,\,2)}=(0.14,\ 0.2,\ 0.26)$	$\tilde{\mu}^3_{(1,\,2)}=(0.16,\ 0.2,\ 0.24)$

B. SENSITIVITY TO FMSS FUZZINESS EXPANSION AND CONTRACTION

Table 5 presents the expansion and contraction parameters settings considered without altering the crisp-value parameters associated with maintenance rates of the three apparatuses. Calculating the FMSS steady-state availability prior to generating the corresponding membership function plot facilitates the investigation of the effect of fuzziness expansion and contraction on FMSS steady-state availability. Fig. 12 depicts the FMSS availability plot revealing an expansion in FMSS-availability fuzziness when using TFN-parameter settings corresponding to the red trend. Conversely, the said fuzziness contracts when using TFN-parameter settings corresponding to the green trend. The ramifications of this result are consistent with mathematical inference.

C. SENSITIVITY WITH RESPECT TO ALTERATION OF DIESEL-GENERATOR DEGRADATION AND MAINTENANCE RATES

Table 6 lists the altered parameter settings for the diesel-generator apparatus, whereas Fig. 13 displays the results of this sensitivity analysis in terms of the steady-state FMSS availability. As can be observed, the better circumstance (green trend) with a small fuzzy interval outperforms the worse circumstance indicated (red trend). The FMSS availability corresponding to the original setting (blue trend) falls between the green and red trends.

TABLE 6. Altered TFN parameters settings to simulate better and worse circumstances for diesel generator apparatus.

Worse circumstance $\lambda \times 1.1$ and $\mu \times 0.9$	Better circumstance $\lambda \times 0.9$ and $\mu \times 1.1$
Diesel generator:	Diesel generator:
$\tilde{\lambda}^3_{(2,\,1)} = (0.011,\ 0.022,\ 0.033)$	$\tilde{\lambda}^3_{(2,\,1)} = (0.009,\ 0.018,\ 0.027)$
$\tilde{\lambda}^3_{(3,\,2)} = (0.022,\ 0.033,\ 0.044)$	$\tilde{\lambda}^3_{(3,\,2)} = (0.018,\ 0.027,\ 0.036)$
$\tilde{\mu}^3_{(1,\,2)} = (0.165,\ 0.22,\ 0.275)$	$\tilde{\mu}^3_{(1,\,2)} = (0.165,\ 0.22,\ 0.275)$
$\tilde{\mu}^3_{(2,\,3)} = (0.18,\ 0.27,\ 0.36)$	$\tilde{\mu}^3_{(2,\,3)} = (0.22,\ 0.33,\ 0.44)$

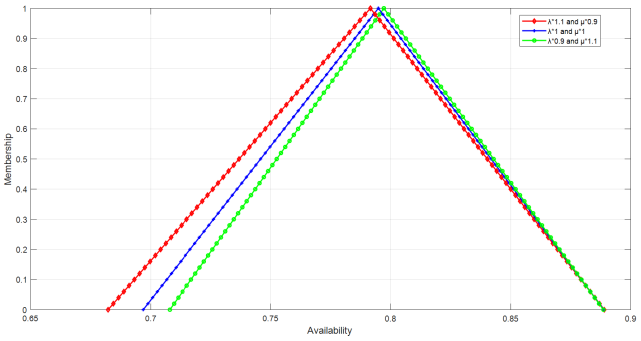

FIGURE 13. Improved steady-state FMSS availability considering altered degradation and maintenance rates of diesel-generator apparatus.

Therefore, the TFN parameter settings considered in this analysis for the diesel generator reflects the extent to which the non-probabilistic uncertainty affects the FMSS availability of the entire community-based smart grid.

VI. CONCLUSION

This paper presents an improved FMSS availability index by establishing a constrained nonlinear parameter-programming model that aims to address the shortcomings of previously proposed indices. These include the violation of the normal convex set principle and contradiction of crisp FMSS availability at α-cut = 1 beyond summation over FMSS probabilities not equal to unity. The case study of a community-based smart-grid system with three FMSCs—solar- and wind energy as well as diesel-generator apparatuses—was considered to verify the efficacy of the proposed approach. The proposed improved FMSS availability index offers the following advantages.

(1) Compliance of FMSS-availability TFNs with the normal convex set principle in fuzzy theory.

(2) The improved FMSS availability with its α-cut level equal to 1 conforms to the MSS availability of crisp observations. Furthermore, the summation over state probabilities equals 1 when the FMSS availability is determined through a normalization procedure.

(3) The three-dimensional plot that depicts the improved FMSS-availability offers further insight into the relationship between the availability, time, and circumstance fuzziness. This plot is expected to help engineers use the availability trajectory to plan and establish appropriate maintenance strategies, thereby making subsequent upgrades more efficient to facilitate the sustainable development of cost-effective and eco-friendly renewable energy.

As a future endeavor, the authors propose to analyze the aging of the apparatus during power plant life cycles by applying the non-homogeneous Markov model in fuzzy circumstances.

REFERENCES

[1] J. Qin and Z. Li, "Reliability and sensitivity analysis method for a multi-state system with common cause failure," *Complexity*, vol. 2019, pp. 1–8, May 2019, doi: 10.1155/2019/6535726.

[2] K. Zhou, J. Ding, J. Chen, and W. Tao, "Reliability and component importance analysis of substation automation system in multi-state mode," *Electr. Power Compon. Syst.*, vol. 47, nos. 6–7, pp. 589–604, Apr. 2019, doi: 10.1080/15325008.2019.1602686.

[3] J. Duan, N. Xie, and L. Li, "Modelling and evaluation of multi-state reliability of repairable non-series manufacturing system with finite buffers," *Adv. Mech. Eng.*, vol. 11, no. 6, pp. 1–13, Jun. 2019, doi: 10.1177/1687814019855483.

[4] A. Lisnianski, I. Frenkel, and L. Khvatskin, "On birnbaum importance assessment for aging multi-state system under minimal repair by using the L_z-transform method," *Rel. Eng. Syst. Saf.*, vol. 142, pp. 258–266, Oct. 2015, doi: 10.1016/j.ress.2015.05.006.

[5] T. Kaul, T. Meyer, and W. Sextro, "Modeling of complex redundancy in technical systems with Bayesian networks," in *Proc. 3rd Eur. Conf. Prognostics Health Manage. Soc.*, 2016, pp. 1–9.

[6] Y. Fang, W. Tao, and K. F. Tee, "Time-domain multi-state Markov model for engine system reliability analysis," *Mech. Eng. J.*, vol. 3, no. 3, pp. 1–14, 2016, doi: 10.1299/mej.16-00084.

[7] M. H. K. Manesh, M. P. Rad, and M. A. Rosen, "New procedure for determination of availability and reliability of complex cogeneration systems by improving the approximated Markov method," *Appl. Thermal Eng.*, vol. 138, pp. 62–71, Jun. 2018, doi: 10.1016/j.applthermaleng.2018.04.042.

[8] A. Lisnianski, "L_z-transform for a discrete-state continuous-time Markov process and its application to multi-state system reliability," in *Recent Advances in System Reliability. Signatures, Multi-state Systems and Statistical Inference*. London, U.K.: Springer, 2012, pp. 79–95, doi: 10.1007/978-1-4471-2207-4_6.

[9] I. Frenkel, A. Lisnianski, L. Khvatskin, A. Karagrigoriou, and A. Kleyner, "On L_z-transform application for availability assessment of aging multi-state water cooling system for medical equipment," in *Applied Reliability Engineering and Risk Analysis: Probabilistic Models and Statistical Inference*. Chichester, U.K.: Wiley, 2013, pp. 59–77.

[10] Y. Ding and A. Lisnianski, "Fuzzy universal generating functions for multi-state system reliability assessment," *Fuzzy Sets Syst.*, vol. 159, no. 3, pp. 307–324, Feb. 2008, doi: 10.1016/j.fss.2007.06.004.

[11] Y. Liu and H.-Z. Huang, "Reliability assessment for fuzzy multi-state systems," *Int. J. Syst. Sci.*, vol. 41, no. 4, pp. 365–379, Apr. 2010, doi: 10.1080/00207720903042939.

[12] L. Hu, D. Yue, and R. Tian, "Fuzzy availability assessment for a repairable multistate series-parallel system," *Discrete Dyn. Nature Soc.*, vol. 2015, pp. 1–11, Jan. 2015, doi: 10.1155/2015/156059.

[13] L. Hu, Z. Zhang, P. Su, and R. Peng, "Fuzzy availability assessment for discrete time multi-state system under minor failures and repairs by using fuzzy L_z-transform," *Eksploatacja i Niezawodnosc*, vol. 19, no. 2, pp. 179–190, 2017, doi: 10.17531/ein.2017.2.5.

[14] Y. Javid, M. A. Ardakan, M. Yaghtin, and M. N. Juybari, "A novel algorithm for estimating reliability of ready-to-use systems in designing phase for designed lifetime based on Markov method and fuzzy approach," *Int. J. Supply Oper. Manage.*, vol. 54, no. 4, pp. 289–297, Jan. 2018, doi: 10.22034/2018.4.1.

[15] P. Gao, L. Xie, W. Hu, C. Liu, and J. Feng, "Dynamic fuzzy reliability analysis of multistate systems based on universal generating function," *Math. Problems Eng.*, vol. 2018, pp. 1–8, May 2018, doi: 10.1155/2018/6524629.

[16] W. Dong, S. Liu, Q. Zhang, R. Mierzwiak, Z. Fang, and Y. Cao, "Reliability assessment for uncertain multi-state systems: An extension of fuzzy universal generating function," *Int. J. Fuzzy Syst.*, vol. 21, no. 3, pp. 945–953, Apr. 2019, doi: 10.1007/s40815-018-0552-x.

[17] H. Wang, F. Duan, and J. Ma, "Reliability analysis of complex uncertainty multi-state system based on Bayesian network," *Eksploatacja i Niezawodnosc*, vol. 21, no. 3, pp. 419–429, 2019, doi: 10.17531/ein.2019.3.8.
[18] L. Hu, D. Yue, and G. Zhao, "Reliability assessment of random uncertain multi-state systems," *IEEE Access*, vol. 7, pp. 22781–22789, Feb. 2019, doi: 10.1109/ACCESS.2019.2898912.
[19] H. Gao and X. Zhang, "A novel reliability analysis method for fuzzy multi-state systems considering correlation," *IEEE Access*, vol. 7, pp. 153194–153204, Oct. 2019, doi: 10.1109/ACCESS.2019.2948497.
[20] A. Roy and K. Chatterjee, "Availability estimation of a multi-state wind farm in fuzzy environment," *Int. J. Green Energy*, vol. 15, no. 2, pp. 80–95, Jan. 2018, doi: 10.1080/15435075.2018.1423977.
[21] H. W. Kuhn and A. W. Tucker, "Nonlinear programming," in *Proc. 2nd Berkeley Symp.*, Berkeley, CA, USA, 1951, pp. 481–492.
[22] L. A. Zadeh, "Fuzzy sets," *Inf. Control*, vol. 8, no. 3, pp. 338–353, 1965, doi: 10.1016/S0019-9958(65)90241-X.
[23] L. A. Zadeh, "Fuzzy sets as a basis for a theory of possibility," *Fuzzy Sets Syst.*, vol. 100, no. 1, pp. 9–34, Jun. 1999, doi: 10.1016/S0165-0114(99)80004-9.
[24] I. A. Ushakov, "A universal generating function," *Sov. J. Comput. Syst. Sci.*, vol. 24, no. 5, pp. 118–129, Sep. 1986.
[25] L. Schulz and D. Schulz, "Numerical analysis of the transient behavior of the non-equilibrium quantum liouville equation," *IEEE Trans. Nanotechnol.*, vol. 17, no. 6, pp. 1197–1205, Nov. 2018, doi: 10.1109/TNANO.2018.2868972.
[26] Q. Yue, L. Zhang, B. Yu, L. J. Zhang, and J. Zhang, "Two-sided matching for triangular intuitionistic fuzzy numbers in smart environmental protection," *IEEE Access*, vol. 7, pp. 42426–42435, Mar. 2019, doi: 10.1109/ACCESS.2019.2906560.
[27] S. Shamshirband, T. Rabczuk, and K.-W. Chau, "A survey of deep learning techniques: Application in wind and solar energy resources," *IEEE Access*, vol. 7, pp. 164650–164666, Nov. 2019, doi: 10.1109/ACCESS.2019.2951750.

GUAN-LIANG CHEN was born in Kaohsiung, Taiwan, in 1983. He received the master's degree in engineering from the National Kaohsiung University of Science and Technology, in 2016. He is currently pursuing the Ph.D. degree with the Chung Cheng Institute of Technology, National Defense University, Taoyuan, Taiwan. His current interests include FMSS reliability analysis and operations research.

CHUN-HO WANG is currently a Professor with the Department of Power Vehicle and Systems Engineering, Chung Cheng Institute of Technology, National Defense University, Taoyuan, Taiwan. He has published several journal articles in the areas of reliability engineering and operation research.

CHAO-HUI HUANG is currently an Associate Professor with the Department of Applied Science, R.O.C. Naval Academy, Kaohsiung, Taiwan. His research interests include the reliability analysis, operations research, and optimization.